ACS APPLIED MATERIALS & INTERFACES

Research Article

www.acsami.org

Novel and Mild Synthetic Strategy for the Sulfonic Acid Functionalization in Periodic Mesoporous Ethenylene-Silica

Manickam Sasidharan[†,‡] and Asim Bhaumik*[,§]

[†]Department of Chemistry, Faculty of Science and Engineering, Saga University, 1 Honjo-machi, Saga 840-8502, Japan

[‡]SRM Research Institute, SRM University, Kattankulathur, Chennai 602 203, India

[§]Department of Materials Science, Indian Association for the Cultivation of Science, Jadavpur, Kolkata -700032, India

ABSTRACT: A new postsynthetic method has been developed for sulfonic acid functionalization of hybrid periodic mesoporous organosilica (PMO) materials containing carbon−carbon double bonds (−C═C−) located in mesoporous wall structures. Hexagonal mesoporous ethenylene-silicas (HME) with different pore sizes were synthesized by using P123, Brij76, and Brij56 surfactants and investigated for postsynthetic functionalization. The present functionalization strategy involves epoxidation of double bonds at −5 °C followed by conversion of the resulting epoxide with bisulfite ions at 65 °C and involves neither the use of well-known mercaptol/H_2O_2 nor harsh concentrated H_2SO_4 reagents during the course of −C═C− functionalization. The epoxidation step plays a crucial role in determining the amount of $-SO_3H$ groups functionalized onto the silica support which is optimized with respect to different synthesis parameters. The ethenylene-silicas both before and after chemical modification were thoroughly characterized by powder XRD, TEM, N_2 adsorption, Raman spectroscopy, ^{13}C and ^{29}Si MAS NMR, and catalytic test reactions. X-ray powder diffraction measurements and sorption data indicated that the mesostructure was intact during the postsynthetic chemical modification. Raman spectra exhibited two strong bands at 1567 and 1290 cm^{-1} for ethenylene-silica attributed to −C═C and −C−H stretching vibrations, respectively; whereas after epoxidation and sulfonation, new bands were observed at 1215 and 1035 cm^{-1} corresponding to the epoxide and $-SO_3$ stretching vibrations, respectively. ^{13}C CP MAS NMR of surfactant extracted ethenylene-silica exhibits a signal at 146 ppm along with signals at 16.4 and 17.4 ppm. The appearance of new signals at 47.7 and 46.5 ppm is attributed to carbon atom with ≡C−OH and ≡C−SO_3H groups, respectively. ^{29}Si MAS NMR spectra exclusively showed T^2 and T^3 species at −73 and −82 ppm, respectively both before and after chemical modification and negligible amount of Q^3 or Q^4 species confirms the stability of Si−C bonds during the functionalization. The sulfonic acid-functionalized mesoporous ethenylene-silicas show high catalytic activity in esterification of acetic acid with ethanol under liquid-phase reaction conditions.

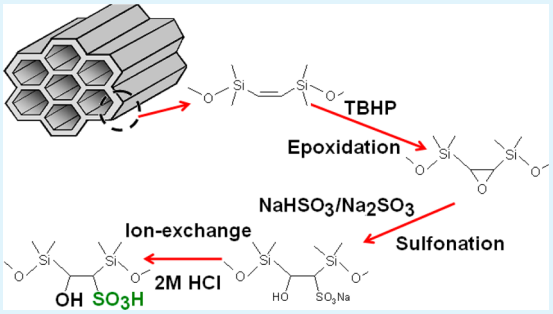

KEYWORDS: *periodic mesoporous organoslica (PMO), sulfonic acid functionalization, heterogeneous catalysis, surface acidity, esterification*

INTRODUCTION

Combining organic and inorganic moieties on multiple-length scales to create functional hybrid materials is receiving a great deal of attention recently.[1,2] These hybrid materials with reactive organic moieties located in the void space of the material offer opportunities for additional modification via reaction of the organic group, but many of them suffer from the occupation of channel space and inhomogeneities associated with the synthesis of materials. The discovery of periodic mesoporous organosilicas (PMOs)[3−5] by using bridged silsesquioxane precursors $(R'O)_3Si-R-(OR')_3$ (where R and R′ are organic groups) and supramolecular templating synthetic approach opened a wide range of new opportunities for designing hybrid materials with controlled surface properties at the molecular level. The organic functionalities bridging the mesoporous framework do not block the pore mouth and can endow PMOs with attractive properties like uniformly distributed organic functionalities in the mesostructure, tunable surface hydrophobicity/hydrophilicity, and mechanical and hydrothermal stabilities compared to conventional mesoporous silica supports. A variety of PMOs with organic spacers R originating from methane, ethane, ethylene, acetylene, butane, benzene, biphenyl, toluene, xylene, imines, thiophene, and ferrocene have been attempted and successfully synthesized in majority of cases.[6−25] Engineering the hydrophobic part of the organic−inorganic hybrid materials by postsynthetic chemical modification assured the materials with specific attributes such as binding sites, Brönsted acidity, and charge density.[26−28]

Today the design of highly accessible and strongly Brönsted acidic mesostructured solids is an area of significant interest in sustainable catalysis.[29] Design of catalysts with high acid strength coupled with good chemical and thermal stability and

Received: January 4, 2013
Accepted: March 13, 2013
Published: March 13, 2013

ready accessibility of the active sites would be a major step forward. The covalent attachment of alkylsulfonic acid groups to the surface of MCM-41/48 and HMS molecular sieves via secondary as well as one-pot co-condensation synthesis methods has been reported.[30−32] To increase the concentration of the $-SO_3H$ groups, one-pot synthetic strategy based on the hydrolysis followed by co-condensation of tetraehoxysilane and (3-mercaptopropyl) trimethoxysilane and in situ oxidation of thiol groups by H_2O_2 in aqueous acidic solution has been proposed.[33] Alternatively, the concentration of sulfonic acid was increased through surface modification with graft polymer containing SO_3H groups.[34,35] In addition, arene sulfonic acids have been prepared by nonoxidative route but the products are reported to be water sensitive and undergo desulfonylation readily.[36,37] Recently, the sulfonated derivatives of various periodic mesoporous organosilicas (PMOs) were also successfully prepared for possible applications in the fields of catalysis as well as solid electrolytes for fuel cells because of the high concentration of acid sites and its strength.[38−42]

Mesoporous ethenylene-silicas have been shown to undergo reactions such as bromination, hydroboration, and alcoholysis.[43−45] So far, investigation of the PMOs indicate that even though bridging functional organic groups are available for reaction but appear to be less reactive than terminally attached functional groups due to steric and electronic differences.[4] Recently, Kondo et al.[46] have prepared highly active and stable ethenylene-silica functionalized with sulfonic acid by post-synthetic modification through Diels−Alder reaction with benzocyclobutene and subsequent sulfonation with conc. H_2SO_4. Very recently, we have reported a dual functionalization of hexagonal mesoporous ethylene silica and their bifunctional catalytic activity.[47]

Here we report a new general method of covalent attachment of sulfonic acid on the surface and channels of periodic mesoporous ethenylene-silica by postsynthetic chemical modification. The present strategy comprises epoxidation of −C═C− bonds of ethylene-silica with appropriate oxidant under mild conditions followed by reaction with sulfite ions[48] to obtain $-SO_3H$ functionalized analogue. It is noteworthy to mention that unlike materials obtained by the common methods where $-SO_3H$ groups are linked through organic spacer, in the present strategy, however, the $-SO_3H$ groups are grafted without any organic spacer. Also, the current synthetic protocol neither involves H_2O_2 nor conc. H_2SO_4. It is also important to note that the epoxy-silica material could serve as a versatile intermediate for preparation of a variety of nanostructured catalytic materials. For example, the epoxide can be treated with NH_3 to obtain amine-functionalized hybrid materials. Alternatively, the epoxide-silica can be hydrolyzed to secondary-alcohol groups that can be further converted to very strong base-catalysts by converting them to alkoxide-groups. In the current study, we have demonstrated the conversion of epoxide in to sulfonic acid by treating with a mixture of $NaHSO_3$ and Na_2SO_3. The chemically modified materials were thoroughly characterized by powder XRD, Raman spectra, ^{29}Si and ^{13}C MAS NMR, sorption and surface area measurements, proton conductivity, and catalytic test reactions. The sulfonic acid modified materials are found to be very active in the esterification of acetic acid with ethanol under liquid-phase conditions.

EXPERIMENTAL SECTION

The triblock copolymer P123, poly(ethylene glycol)-block-poly-(propylene glycol)-block-poly(ethylene glycol) (PEG-PPG-PEG); M_w 5800), oligomeric surfactants Brij 76 ($C_{18}EO_{10}$) and Brij 56 ($C_{16}H_{33}(OCH_2CH_2)_{10}OH$) were obtained from Aldrich. The silica source Bis(triethoxysilyl)ethylene (BTSE, 95%) was obtained from GELEST, INC. The oxidizing agents aqueous H_2O_2 (30−35%, Wako), tert-butylhydroperoxide solution anhydrous (TBHP, 5.5 M in decane, dried over molecular sieve 4A, Fluka), and 3-chloroperbenzoic acid (77%, Aldrich) were obtained commercially. Sodium sulfite (97%, Wako), sodium bisulfite (99%, Sigma-Aldrich), and NaCl (99.5%, Nacalai tesque) were also purchased from commercial source.

Preparation of Hexagonal Mesoporous Ethenylene-Silica Using P123 Polymer. In a typical synthesis of hybrid mesoporous ethenylene-silica, 3.0 g of P123 was added to 67 mL of ion-exchanged water and 45 mL of 4 M HCl and dissolved by stirring at room temperature. To the above solution was added 5.55 g of BTSE and the contents were stirred at 40 °C for 24 h. The resulting mixture with white precipitate was then transferred to polypropylene bottle and heated at 100 °C for an additional 24 h under static conditions. The solid product was filtered, washed thoroughly with water and ethanol. The polymeric surfactant was removed by refluxing 1 g of as-synthesized material with 200 mL of ethanol and 5 mL of 4 M HCl solution for 20 h and this process was repeated twice. Finally the solid was filtered, washed with copious amount of water and ethanol, and finally dried under vacuum of 1×10^{-3} Torr in a desiccator. The resultant material for convenience designated as hexagonal mesoporous ethenylene-silica HME(P123).

Preparation of HMEs in the Presence of Brij 76 and Brij 56 Surfactants. Hexagonal mesoporous ethenylene-silicas were also prepared using Brij 76 and Brij 56 according to the following molar gel composition: BTSE: oligomer: $HCl:H_2O$ = 1:0.27:7.7:53. In a typical preparation, 2 g of Brij 76 was dissolved in 10 mL of ion-exchanged water and 50 mL of 2 M hydrochloric acid at room temperature. After complete dissolution, BTSE (1.85 g) was added, and the mixture was stirred at 50 °C for 20 h, followed by another 24 h heating at 100 °C under static conditions. A white precipitate was recovered by filtration, washed thoroughly with water and ethanol, and finally dried. The oligomeric surfactants were removed by solvent extraction as described previously. For synthesis of HME with Brij 56, 1.92 g of surfactant was used and the synthesis was performed under similar conditions as before. These materials were referred to as HME(Brij76) and HME(Brij56) in subsequent discussion.

Epoxidation of Ethenylene-Silica HME(P123). In a typical epoxidation reaction, 0.25 g of HME(P123) was suspended in 6 mL of dry acetonitrile and 50 mL of 2 M NaOH solution was added under stirring at room temperature and then the content was effectively cooled to −5 °C using freezing mixture (ice/NaCl). Then, 1.5 mL of TBHP was added and the contents were stirred vigorously using a magnetic stirrer for 4.5 h. After the reaction, the solid was filtered, washed thoroughly with acetonitrile and ethanol, and finally dried under a vacuum at 1×10^{-3} Torr for 3 h.

Conversion of Epoxy-Silica in to SO_3H-Silica Using Bisulfite Ions. The dried epoxy-silica was transferred into a round-bottom flask and added 9 mL of $NaHSO_3$ (1.5 mol) and 6 mL of Na_2SO_3 (1.5 mol) ($NaHSO_3$: Na_2SO_3 = 60: 40 ratio). The flask was fitted with water condenser to circulate cold water during the reaction. The reaction mixture was stirred at 40 °C for overnight and after the completion of reaction, the white solid was filtered, washed thoroughly with a large amount of water to remove the occluded sulfite ions to obtain material with covalently attached $-SO_3Na$ groups. The resultant material was ion-exchanged with 2 M HCl by stirring at room temperature for 20 h to get $-SO_3H$ functionalized ethylene-silica.

Esterification of Acetic Acid with Ethanol over SO_3H-HME. In a typical reaction of esterification, 30 mL of ethanol was mixed with 2.86 mL of acetic acid in a round-bottom flask. To the above mixture 0.1 g of preactivated (activated under vacuum at 100 °C for 1 h) SO_3H-HME was added. The reaction flask was fitted with water condenser and the reaction was carried out by stirring the reaction mixture vigorously using magnetic stirrer at 70 °C for 24 h. The

reaction products were analyzed using gas chromatography fitted with FID detector and the formation of ester was confirmed using authentic sample. The quantification of the product was done using toluene as an internal standard.

CHARACTERIZATION TECHNIQUE

Powder X-ray diffraction (PXRD) patterns were measured on a Rigaku RINT-2200 diffractometer with CuKα radiation (40 kV, 30 mA) from 0.7 to 8° (2θ) in 0.01 steps at a scan speed of 1°(2θ) min^{-1}. The morphology of the sample was confirmed by transmission electron microscope observation (JEOL-2000EXII, 200 kV) and field emission SEM (Hitachi S-800). Porosimetry measurements (N_2 isotherms) were obtained on a Quantachrome Autosorb-1 sorptometer at −196 °C. Prior to measurement, all samples were outgassed at 60 °C and 1 × 10^{-4} Torr for 3 h. Brunauer−Emmett−Teller (BET) surface areas were calculated from the linear section of the BET plot (P/P_0 = 0.05−0.2). Pore-size distributions were determined using the Barrett−Joyner−Halenda (BJH) method from the adsorption branch of the isotherms. The ^{29}Si MAS NMR and ^{13}C CP MAS NMR spectra were recorded on a Bruker MSL-300WB spectrometer at 59.62 and 75.47 MHz for ^{29}Si and ^{13}C, respectively. Their chemical shifts were referenced to tetramethylsilane and glycine, respectively. Raman spectra were obtained using the 532 nm laser line with a JASCO micro-Raman system NRS-3300 equipped with holographic notch filter, 600 grooves/mm holographic grating, a 100×-microscope objective, and a peltier cooled (−50 °C) CCD detector. FTIR spectra were recorded using powder samples on a Shimadzu FTIR-8100 spectrometer using ATR method. The acid-catalyzed reaction products were analyzed using Shimadzu 8A gas chromatograph equipped with FID detector.

RESULTS AND DISCUSSION

The structural ordering of HMEs (hexagonal mesoporous ethenylene-silicas) with different pore sizes was assessed by powder XRD. Figure 1 shows the XRD patterns for the various samples after surfactant extraction. The samples (Figure 1a, c, e) before chemical modification exhibit (100), (110), and (200) reflections characteristic of hexagonal p6mm symmetry indicating a highly ordered hexagonal phase with homogeneous distribution of bridging ethenylene groups. All the samples both before and after $-SO_3H$ functionalization exhibited strong diffraction peak below $2\theta \approx 1°$, which correspond to the (100) reflection of 2D hexagonal unit cells. For the materials synthesized with P123 and Brij76 surfactants showed well-resolved diffraction peaks for (110) and (200) reflections; however these reflections are relatively less intense for sample synthesized with Brij56. The structural properties of various ethenylene-silica before and after postsynthetic chemical modification are listed in the Table 1. From Figure 1b, d, and f, it is seen that postsynthetic chemical modification of ethenylene-silica does not affect the mesostructural ordering. However, after sulfonic acid functionalization the unit-cell volume decreases slightly.

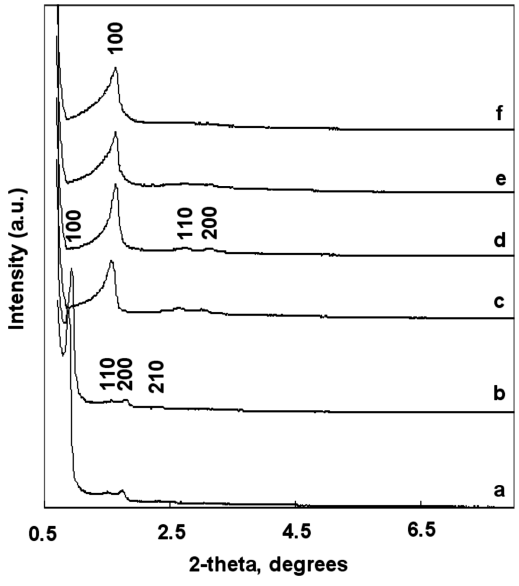

Figure 1. PXRD patterns of extracted ethenylene-silica (HME) synthesized with different surfactants: (a) HME(P123), (b) HME-(P123)−SO_3H, (c) HME(Brij76), (d) HME(Brij76)−SO_3H, (e) HME(Brij56), and (f) HME(Brij56)−SO_3H.

Figure 2 shows the TEM image of HME(P123) sample, where 2D-hexagonal mesophase and honeycomb like arrangement of the pore channels are quite clear. SEM observation reveals spherical particles of size <1 μm for HME(P123) and 2−3 μm for HME(Brij76); however, HME(Brij 56) exhibits wheat like morphology with size of about 7 μm. The pore structure of the different ethenylene-silicas were also evaluated by nitrogen sorption studies. The sorption data presented in Figure 3 are characteristic of type IV isotherm based on the International Union of Pure and Applied Chemistry (IUPAC) classification confirming the existence of uniform mesopores.[4−6] The textural properties such as BET surface area, pore volume, and pore wall thickness of different ethenylene-silicas are summarized in Table 1. Ethenylene-silicas prepared in the presence of P123, Brij76, and Brij56 exhibited a steep adsorption uptake due to capillary condensation of nitrogen in the mesopore with narrow pore size distribution (PSD). It is worthy to note that the mesoporosity remains intact after attachment of sulfonic acid by postsynthetic chemical modification as revealed from adsorption data. The mild postsynthetic modification helps to retain majority of mesostructural features. In general the postsynthetic modification leads to decreased BET surface area as well as micropore volume.

Consistent with XRD data, HME(Brij76) and HME(Brij56) exhibit much narrower pore size distributions than the P123-HME as shown in Figure 4. These ethenylene-silicas with different pore sizes were used for functionalization of $-SO_3H$ in the current study.

The present strategy for introduction of sulfonic acid on the surface of ethenylene-silica is presented in Scheme 1 and the epoxidation step plays a crucial role in determining the amount of $-SO_3H$ groups attached to the silica surface. Therefore the epoxidation reaction was optimized with respect to reaction temperature, nature of oxidant used, influences of pH, water content, and reaction time. However, the subsequent conversion of epoxy-silica to the corresponding $-SO_3H$-silica using a mixture of $NaHSO_3$ and Na_2SO_3 is sensitive to the reaction temperature. Finally, the $-SO_3Na$ was ion-exchanged with 2 M HCl for 12 h to obtain the $-SO_3H$. To optimize the synthesis conditions and identify the intermediate species formed during the chemical modification, we analyzed the various samples by Raman spectroscopy. Raman spectra (Figure 5) showed the presence of ethene groups (−C═C−) in surfactant-extracted samples from the observation of

Table 1. Structural Properties of Mesoporous Ethenylene-Silica Samples before and after Sulfonic Acid Functionalization

different HME materials	S_{BET} (m^2 g^{-1})	V (mL g^{-1})	D (nm)	d(100) (nm)	lattice constant (nm)	wall thickness (nm)
HME(P_{123})	845	1.15	8.6	11.1	12.9	4.3
HME(P_{123})-SO_3H	833	1.13	8.3	10.1	11.3	3.0
HME(Brij76)	1240	1.50	3.9	6.38	7.37	3.4
HME(Brij76)-SO_3H	1153	1.25	3.5	6.03	6.96	4.4
HME(Brij56)	1447	1.57	3.7	6.07	7.0	3.3
HME(Brij56)-SO_3H	1220	1.22	3.5	6.03	6.95	3.45

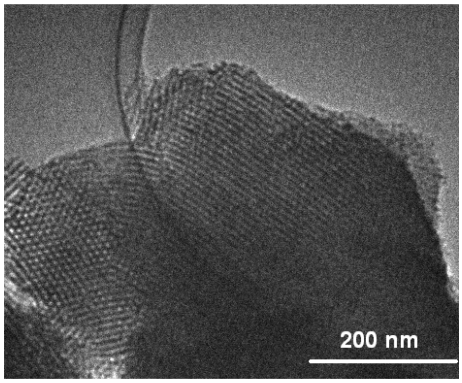

Figure 2. Transmission electron microscopic image of HME(P123).

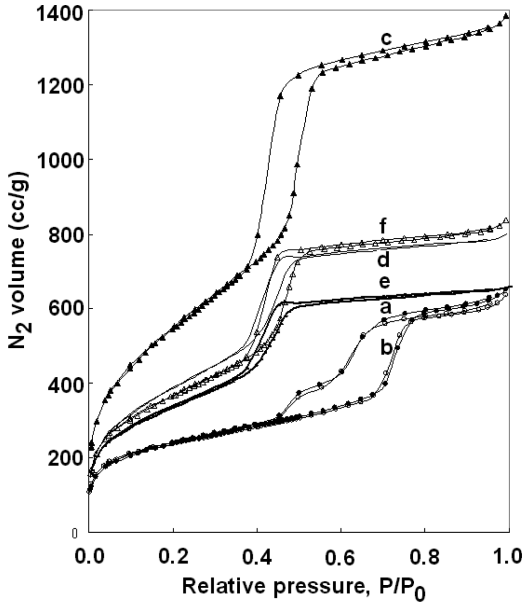

Figure 3. Nitrogen adsorption−desorption isotherms of ethenylene-silicas before and after SO_3H functionalization: (a) HME(P123), (b) HME(P123)-SO_3H, (c) HME(Brij76), (d) HME(Brij76)-SO_3H, (e) HME(Brij56), and (f) HME(Brij56)-SO_3H. *Y*-axis value for c has been enhanced by 150.

two strong bands at 1567 and 1290 cm-1 which can be ascribed to −C═C− and −C−H stretching vibrations, respectively.[4] After epoxidation of ethenylene-silica with TBHP at −5 °C, a new band appears at 1215 cm-1 which is attributed to the formation of epoxide ring stretching vibration.[49] When the epoxide containing materials were treated with sulfite ions, a band at 1035 cm^{-1} attributed to $-SO_3$ stretching vibrations has been noticed.[50] At the same time the band corresponding to the epoxide ring (1215 cm^{-1}) is nearly disappeared indicating an effective conversion of epoxide into sulfonic acid groups.

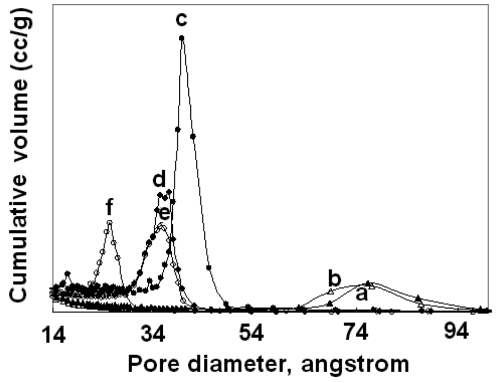

Figure 4. Pore size distribution of ethenylene-silicas before and after sulfonic acid functionalization: (a) HME(P123), (b) HME(P123)-SO_3H, (c) HME(Brij76), (d) HME(Brij76)-SO_3H, (e) HME(Brij56), and (f) HME(Brij56)-SO_3H.

Scheme 1. Schematic Representation of the Sulfonic Acid Functionalization of HMEs

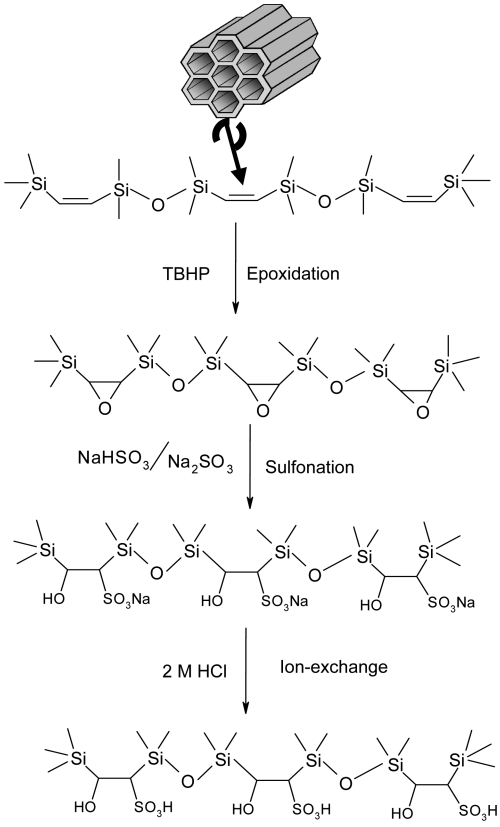

Thus the Raman spectral results clearly prove successful addition of $-SO_3H$ group across the −C═C− bond.

dx.doi.org/10.1021/am4000326 | ACS Appl. Mater. Interfaces 2013, 5, 2618−2625

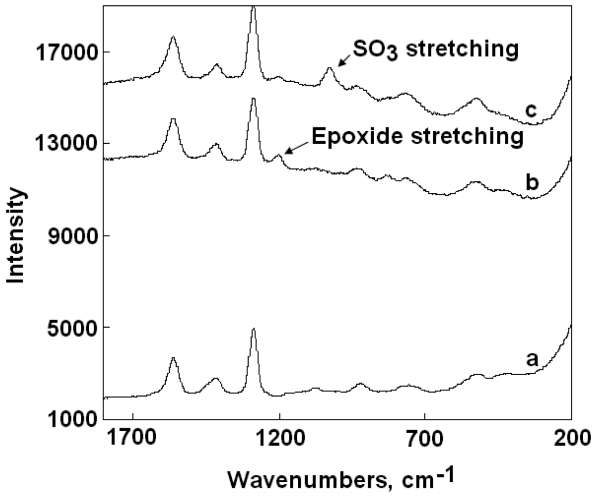

Figure 5. Raman spectra of postsynthetically modified ethenylene-silica: (a) HME(P123), (b) HME(P123) after epoxidation, and (c) HME(P123) with $-SO_3H$ group.

Because the epoxidation plays a crucial role in the current strategy, the reaction was thoroughly scrutinized with various reaction parameters. It is important to note that the amount of ethylene-epoxide formed was estimated indirectly by converting to sulfonic acid which was quantified by potentiometric acid−base titration and therefore under optimized reaction conditions, the amount of sulfonic acid estimated by titration is directly proportional to the amount of epoxide produced. Figure 6A shows the efficiency of various oxidants in the epoxidation of ≡Si−C═C−Si≡ species at −5 °C. Initially we have attempted to epoxidize by using 3-chloroperbenzoic acid as oxidant but the observed results were not satisfactory due to the reason that the double bond bearing carbon atoms are attached to electropositive silicon atom on both side of carbon−carbon double bond. It is well established fact that the rate of epoxidation by electrophilic mechanism decreases as the availability of electron over the double bonds decreases.[51] Thus the electronic factor is not favorable for facile formation of epoxide containing silica using perbenzoic acid. In order to circumvent the electronic factor, we have used a combination of 3-chloroperbenzoic acid (MCPBA) and triethylamine (TEA) under anhydrous conditions which is known to react by nucleophilic mechanism but this strategy also failed to improve the yield of epoxide. The use of a combination of aqueous H_2O_2 and NaOH improved the amount of epoxide formed[52] by nucleophilic pathway but the presence of water in the aqueous H_2O_2 leads to unwanted side reaction which is explained further in the later discussion. Finally the use of anhydrous *tert*-butylhydroperoxide in decane (TBHP) and NaOH resulted in better epoxide yield than the other oxidants under similar experimental conditions as shown in Figure 6A, and therefore, TBHP was used for further study.

Similarly, the epoxidation is also sensitive to the reaction temperature and the amount of epoxide formed at various temperatures is shown in Figure 6B. The ethylene-epoxide is highly unstable at higher temperature particularly above 50 °C under the reaction conditions; whereas the reaction is very sluggish for temperature below −5 °C and even increased reaction time did not enhance the amount of epoxide. The optimum reaction temperature was found to −5 °C and is used in the subsequent experiments. The stability of epoxide species also depends on the reaction duration and the amount of

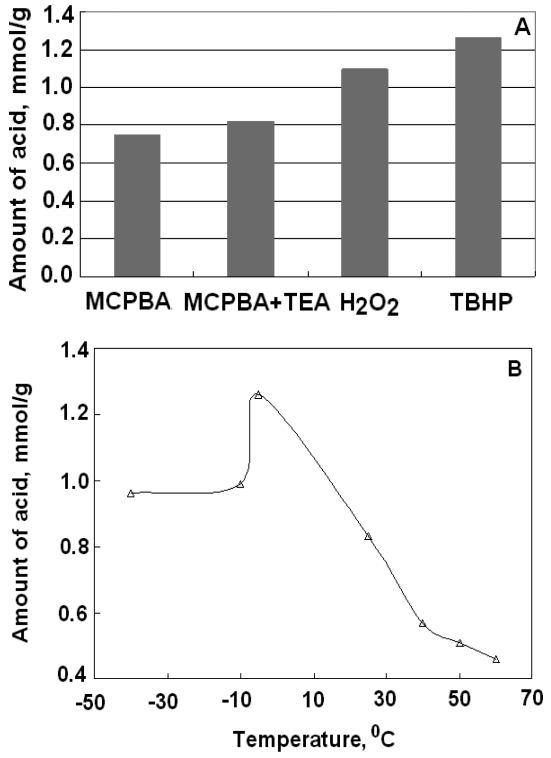

Figure 6. (A) Amount of acid for sulfonated ethenylene-silica prepared with different epoxidation reagents; HME(P123) = 0.25 g, TBHP = 1.5 mL (oxidant/silica mole ratio = 2.6), acetonitrile = 6 mL, temperature = −5 °C, 2 M NaOH solution = 50 μL, reaction time = 4.5 h; and (B) variation of acid-sites density at different temperatures using TBHP as oxidants and the remaining conditions are same as mentioned above.

epoxide formed increases with time and reaches a maximum in 4.5 h and prolonged stirring decreases the amount of epoxide possibly due to cleavage of epoxide ring (Figure 7A). In addition, the pH of the medium also influences reaction rate as well as stability of epoxide species as shown in Figure 7B. The use of pH below 8 fails to accelerate the nucleophilic oxidative epoxidation50 under the reaction conditions. In addition, excess of NaOH also leads to cleavage of epoxide ring to diols by base-catalyzed mechanism.[53] The optimum pH for epoxidation was found to be in the range of 8.5−9.0 for the formation of epoxide.

The amount of water also plays a major role in the epoxidation reaction. For example, the amount of epoxide as well as sulfonic acid formed is directly affected by the amount of water present in the reaction medium. This is mainly due to the direct consequence of the cleavage of epoxide ring to diols as shown in Scheme 2. Thus the presence of water leads to facile formation of diols at the expense of epoxides. The above results clearly demonstrate that the epoxide subsequently undergoes side reaction such as the well-known cleavage of epoxide to diols.[51] Hence all the epoxidation reactions were carried out under optimized reaction conditions unless otherwise mentioned. Reaction between epoxides and sulfur-(IV) ions generally result in ring-opening of epoxide to give sulfonic acids.[54] This reaction has been reported to be a neuleophilic reaction of sulfite ion with epoxide ring, whereas bisulfite ion promotes the epoxide oxygen through protonation. Thus, the reaction has been reported to be facile when a mixture of $NaHSO_3$ and Na_2SO_3 was employed. Hence, in the

dx.doi.org/10.1021/am4000326 | ACS Appl. Mater. Interfaces 2013, 5, 2618−2625

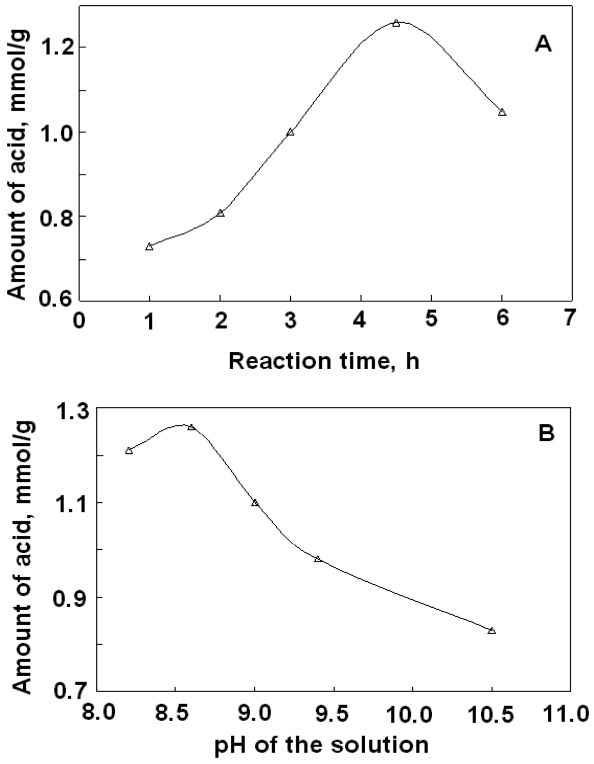

Figure 7. (A) Influence of reaction time over the amount of $-SO_3H$ grafted at the surface of HMEs; HME(P123) = 0.25 g, TBHP = 1.5 mL (oxidant/silica mole ratio = 2.6), acetonitrile = 6 mL, temperature = −5 °C, 2 M NaOH solution = 50 μL; (B) amount of $-SO_3H$ formed at different pH and the pH was adjusted using 0.1 M aqueous NaOH under optimized reaction conditions and the remaining conditions are same as mentioned above.

Scheme 2. Ring-Opening of the Epoxides of HMEs

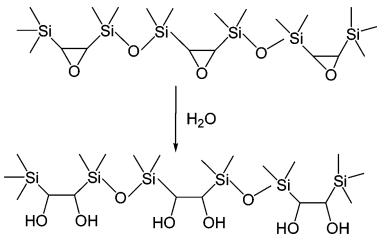

present study we have employed a mixture of $NaHSO_3$ (60%) and Na_2SO_3 (40%) under optimized reaction conditions. Finally, the sodium form of the sulfonic acid was converted to sulfonic acid by ion-exchange with 2 M HCl.

Thus, the concentration of $-SO_3H$ can be maximized by tuning the epoxidation temperature, water content, and sulfonation reaction.The postsynthetic modifications have also been supported by solid-state ^{13}C CP MAS NMR and ^{29}Si MAS NMR data. The ^{13}C CP MAS NMR spectra of surfactant extracted HME(P123) (Figure 8A) had a strong resonance peak at 145.6 ppm corresponding to the ethylene carbon atoms linked to silicon. The additional two signals observed at 57.6 and 15.5 ppm are attributed to nonhydrolyzed Si-OC_2H_5 from silicon source.[4] After epoxidation, the ethenylene-silicas exhibit a new rather broad signal centered at 45.1 ppm and the sulfonated material at 47.7 and 46.5 ppm (see inset figure). The signals at 47.7 and 46.5 ppm (Figure 8C) are assigned to ≡C−OH and ≡C−SO_3H chemical environments, respectively. We

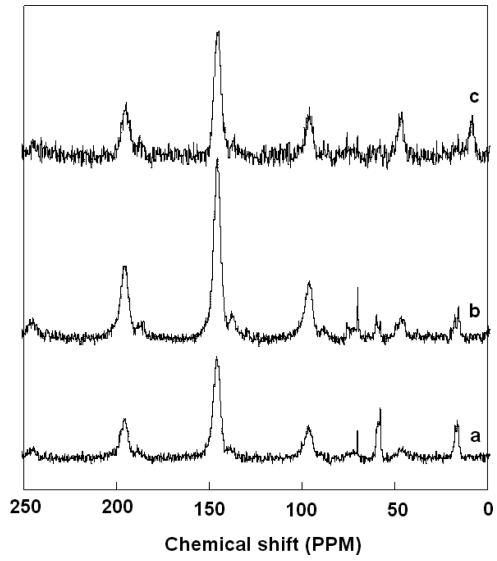

Figure 8. (a) ^{13}C CP MAS NMR spectra of HME(P123), (b) epoxidized-HME(P123), and (c) sulfonated-HME(P123).

have also noted a weak signal at 7.9 ppm corresponding to Si-CH_3 due to symmetrical hydrolysis of Si−C═C−Si bond during sulfonation. In addition, the peak at 145.6 ppm did not vanish completely, indicating that only a fraction of −C═C− bonds were epoxidized and those located probably within the pore walls are inaccessible for epoxidation. The ^{29}Si MAS NMR of surfactant extracted HME(P123) (Figure 9A) exhibits

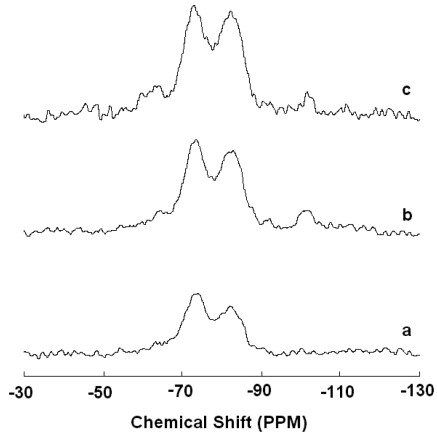

Figure 9. (a) ^{29}Si MAS NMR spectra of HME(P123), (b) epoxidized-HME(P123), and (c) sulfonated-HME(P123).

mostly two prominent signals at −74.5 and −83 ppm, which can be assigned to Si species covalently bonded to carbon atoms of (C═C)−Si−$(OSi)_2(OH)$ (T2 sites) and (C═C)−Si−$(OSi)_3$ (T3 sites), respectively. No Q [Si(OSi)4] silicon sites are seen, indicating that the Si−C bonds remained intact under the synthesis conditions. After epoxidation, the ethenylene-silica shows T2 and T3 sites in addition to very weak signals at −64.4 and −102 ppm (Figure 9B), which can be assigned to (C═C)−Si−$(OSi)(OH)_2$ (T1 sites) and (OH)−Si−$((OSi)_3$ (Q3 sites), respectively.[55] Similar to epoxy-silica, the sulfonic acid attached material also exhibits T2 and T3 signals (Figure 9C). All the materials after chemical modification did not change the T site position; however the intensity of T3 signal slightly increased for epoxy- and

dx.doi.org/10.1021/am4000326 | ACS Appl. Mater. Interfaces 2013, 5, 2618−2625

sulfonated-silicas indicating that mesostructural order is preserved during postsynthetic chemical modification.

Similar to HME(P123) ethenylene-silica, HME(Brij76) and HME(Brij56) with narrow pore sizes were also modified with sulfonic acid and the corresponding ^{13}C CP MAS NMR spectra are shown in Figure 10. The spectra exhibit a signal at 45.8

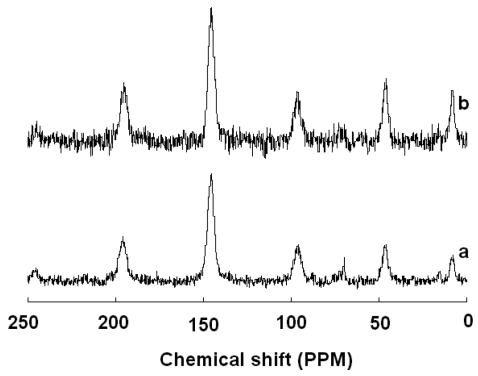

Figure 10. ^{13}C CP/MAS NMR spectra of (a) HME(Brij56)-SO_3H and (b) HME(Brij76)-SO_3H.

ppm, which is supposed to be a doublet but not well resolved, can be assigned to $-SO_3H$ groups covalently attached to carbon atoms. The ^{29}Si MAS NMR of these samples are shown in Figure 11 and exhibits predominantly T^2 and T^3 signals; in

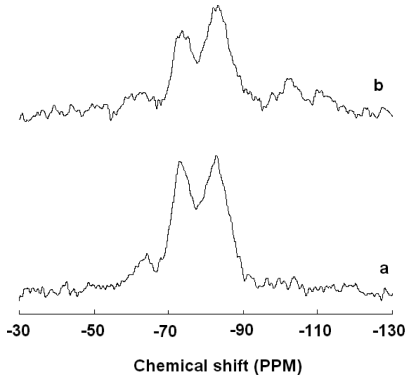

Figure 11. ^{29}Si MAS NMR spectra of (a) HME(Brij56)-SO_3H and (b) HME(Brij76)-SO_3H.

the case of HME(Brij56)-SO_3H, a weak T^1 signal at −64.6 ppm is observed and no Q signals were noted. However, in the case of (HME)Brij76-SO_3H, a signal at −103 ppm attributable to Q^3 species was detected. Among the three ethenylene-silicas with different pore sizes studied, the P123HME with large pore diameter exhibited largest amount of acid sites 1.26 mmol/g than HME(Brij56) and HME(Brij76) samples. From the amount of sulfonic acid attached over HME(P123), it was estimated that 16.3% of −C═C− double bonds were effectively converted into sulfonic acids and the remaining double bonds may be located inside inaccessible pore walls similar to earlier observation.[4]

Further evidence for the sulfonic acid-functionalized periodic mesoporous ethenylene-silica by the current method was obtained from the liquid phase catalytic test reaction. The performance of various catalysts with different pore size in the esterification of acetic acid with ethanol under liquid-phase conditions is shown in the Table 2. The amount of ester

Table 2. Catalytic Activity of Sulfonic Acid Functionalized Mesoporous Ethenylene-Silicas in the Esterifcation of Acetic Acid with Ethanol[a]

			conversion, mole %	
entry	catalyst	acidity (mmol H^+/g)	6 h	24 h
1	HME(P_{123})-SO_3H	1.05	36	83
2	HME(P_{123})-SO_3H	1.26	49	86
3	HME(Brij76)-SO_3H	0.95	36	76
4	HME(Brij56)-SO_3H	0.89	29	66
5[b]	HME(P_{123})-SO_3H	1.26	43	85

[a]Reaction conditions: acetic acid = 2.86 mL, ethanol = 30 mL, catalyst = 0.1 g, reaction temperature = 70 °C. [b]After second recycle of entry 2.

product (ethyl acetate) formed is influenced by the acid-site density of the samples. For example, after 6 h, HME(P123)-SO_3H gave conversion of 49% (entry 2), whereas HME-(Brij56)-SO_3H led to only 29% (entry 4). Interestingly, the esterifcation reaction is governed by acid-site density as revealed from entries 1 and 2. HME(P123)-SO_3H synthesized through TBHP oxidant has higher acid density and thus it showed higher catalytic activity over the same material synthesized by using H_2O_2 as oxidant in the epoxidation step. Further, acidic ion-exchange resin Amberlyst-15 used in this esterification reaction resulted in 79% yield of the ester in the equilibrium reaction mixture.[56] This result suggested that our sulfonic acid functionalized mesoporous materials are comparable to the commercially known acid catalyst for this reaction. However, not much difference has been observed for the saturated conversion level at 24 h. Ethyl acetate is an essential raw material widely used in the chemical industry. Conversion level observed over HME(P123)-SO_3H material is also comparable to that produced in the membrane reactors.[57] It is worth to mention that the catalyst retains the original activity after four cycles of repeated uses (entry 5). Moreover, blank reaction in the absence of any catalyst resulted only 17.0% conversion with equilibrium reached after 4 h reaction time, indicating strong catalytic role of sulfonic acid sites in this esterification reaction.

CONCLUSION

A new functionalization strategy for $-SO_3H$ has been successfully developed for the hybrid periodic mesoporous organosilica materials bearing −C═C− bonds at the bridging organosilane moiety under mild conditions. Among the various steps involved in the postsynthetic chemical modification, the epoxidation of ethenylene-silica plays a crucial role in determining the acid-site density. *tert*-Butylhydroperoxide has been found to be an effective oxidant than the aqueous H_2O_2 or *m*-chloroperbenzoic acid. Reaction parameters such as temperature, pH, amount of water, and reaction time influenced the formation and stability of epoxide. Raman spectroscopy exhibited bands at 1215 and 1035 cm^{-1} confirming the formation of epoxide and $-SO_3H$ groups, respectively. ^{13}C CP MAS NMR spectra showed a resonance signals at 47.7 and 46.5 ppm assigned to ≡C−OH and ≡C−SO_3H chemical environments, respectively. The postsynthetic modification of different ethenylene-silicas with different pore size indicated that P123HME with large pore size showed higher acid site density of 1.26 mmol/g than the Brij76HME (0.95 mmol/g) and Brij56HME (0.89 mmol/g). The sulfonic acid functionalized

PMO catalyst showed good catalytic activity in the esterification of acetic acid with ethanol under liquid-phase reaction conditions.

AUTHOR INFORMATION

Corresponding Author

*E-mail: msab@iacs.res.in (A.B.); sasidharan.m@res.srmuniv.ac.in (M.S.).

Notes

The authors declare no competing financial interest.

ACKNOWLEDGMENTS

A.B. thanks DST New Delhi for providing instrumental facility through Nano Mission Initiative. M.S. thanks Dr. S. Inagaki for helpful discussions.

REFERENCES

(1) Mann, F. *Nature* **1993**, *365*, 499.
(2) Li, Q. F.; Zeng, L. X.; Wang, J. C.; Tang, D. P.; Liu, B. Q.; Chen, G. N.; Wei, M. D. *ACS Appl. Mater. Interfaces* **2011**, *3*, 1366−1373.
(3) Inagaki, S.; Guan, S.; Fukushima, Y.; Ohsuna, T.; Terasaki, O. *J. Am. Chem. Soc.* **1999**, *121*, 9611.
(4) Asefa, T.; MacLachlan, M. J.; Coombs, N.; Ozin, G. A. *Nature* **1999**, *402*, 867.
(5) Melde, B. J.; Holland, B. T.; Blanford, C. F.; Stein, A. *Chem. Mater.* **1999**, *11*, 3302.
(6) Bhaumik, A.; Kapoor, M. P.; Inagaki, S. *Chem. Commun.* **2003**, 470−471.
(7) Hao, N.; Yang, Y. X.; Wang, H. T.; Webley, P. A.; Zhao, D. Y. *J. Colloid Interface Sci.* **2010**, *346*, 429−435.
(8) Chandra, D.; Yokoi, T.; Tatsumi, T.; Bhaumik, A. *Chem. Mater.* **2007**, *19*, 5347−5354.
(9) Wang, W.; Zhou, W.; Sayari, A. *Chem. Mater.* **2003**, *15*, 4886.
(10) Chandra, D.; Das, S. K.; Bhaumik, A. *Microporous Mesoporous Mater.* **2010**, *128*, 34−40.
(11) Keilbach, A.; Doeblinger, M.; Koehn, R.; Amenitsch, H.; Bein, T. *Chem.—Eur. J.* **2009**, *15*, 6645−6650.
(12) Wu, K. C. −W.; Yamauchi, Y. *J. Mater. Chem.* **2012**, *22*, 1251−1256.
(13) Matos, J. R.; Kruk, M.; Mercuri, L. P.; Jaroniec, M.; Asefa, T.; Coombs, N.; Ozin, G. A.; Kamiyama, T.; Terasaki, O. *Chem. Mater.* **2002**, *14*, 1903.
(14) Lu, Y.; Fan, H.; Doke, N.; Loy, D. A.; Assink, R. A.; LaVan, D. A.; Brinker, C. J. *J. Am. Chem. Soc.* **2000**, *122*, 5258.
(15) Fulvio, P. F.; Brosey, R. I.; Jaroniec, M. *ACS Appl. Mater. Interfaces* **2010**, *2*, 588−593.
(16) Sayari, A.; Hamoudi, S.; Yang, Y.; Moudrakovski, I. L.; Ripmeester, J. R. *Chem. Mater.* **2000**, *12*, 3857.
(17) Nguyen, T. P.; Hesemann, P.; Moreau, J. J. E. *Microporous Mesoporous Mater.* **2011**, *142*, 292−300.
(18) Kruk, M.; Jaroniec, M.; Guan, S.; Inagaki, S. *J. Phys. Chem. B* **2001**, *105*, 681.
(19) Zhu, F. X.; Wang, W.; Li, H. X. *J. Am. Chem. Soc.* **2011**, *133*, 11632−11640.
(20) Modak, A.; Mondal, J.; Aswal, V. K.; Bhaumik, A. *J. Mater. Chem.* **2010**, *20*, 8099−8106.
(21) Huang, J. L.; Zhang, F.; Li, H. X. *Appl. Catal. A: Gen.* **2012**, *431*, 95−103.
(22) Hamoudi, S.; Kaliaguine, S. *Chem. Commun.* **2002**, 2118.
(23) Tucker, M. H.; Crisci, A. J.; Wigington, B. N.; Phadke, N.; Alamillo, R.; Zhang, J. P.; Scott, S. L.; Dumesic, J. A. *ACS Catal.* **2012**, *2*, 1865−1876.
(24) Nohair, B.; Phan, T. H. T.; Vu, T. H. N.; Tien, P. Q.; Phuong, D. T.; Hy, L. G.; Kaliaguine, S. *J. Phys. Chem. C* **2012**, *116*, 10904−10912.
(25) Yamauchi, Y.; Suzuki, N.; Gupta, P.; Sato, K.; Fukata, N.; Murakami, M.; Shimizu, T.; Inoue, S.; Kimura, T. *Sci. Technol. Adv. Mater.* **2009**, *10*, 025005.
(26) Ying, J. Y.; Mehnert, C. P.; Wong, M. S. *Angew. Chem., Int. Ed.* **1999**, *38*, 56.
(27) Kickelbick, G. *Angew. Chem., Int. Ed.* **2004**, *43*, 3102.
(28) Valenstein, J. S.; Kandel, K.; Melcher, F.; Slowing, I. I.; Lin, V. S. -Y.; Trewyn, B. G. *ACS Appl. Mater. Interfaces* **2012**, *4*, 1003−1009.
(29) Sasidharan, M.; Bhaumik, A. *J. Sol−Gel Sci. Technol.* **2012**, *61*, 367−373.
(30) Van Rhijn, W. M.; De Vos, D. E.; Sels, B. F.; Bossaert, W. D.; Jacobs, P. A. *Chem. Commun.* **1998**, 317.
(31) Lim, M. H.; Blanford, C. F.; Stein, A. *Chem. Mater.* **1998**, *10*, 467.
(32) Bossaert, W. D.; De Vos, D. E.; Van Rhijn, W. M.; Bullen, J.; Grobet, P. J.; Jacobs, P. A. *J. Catal.* **1999**, *182*, 156.
(33) Margolese, D.; Melero, J. A.; Christansen, S. C.; Chmelka, B. F.; Stucky, G. D. *Chem. Mater.* **2000**, *12*, 2448.
(34) Li, C.; Yang, J.; Wang, P.; Liu, J.; Yang, Q. *Microporous Mesoporous Mater.* **2009**, *23*, 228.
(35) Martin, A.; Morales, G.; Martinez, F.; Grieken, R.; van Cao, L.; Kruk, M. *J. Mater. Chem.* **2010**, *20*, 8026.
(36) Melero, J. A.; Stucky, G. D.; Van Grieken, R.; Morales, G. J. *J. Mater. Chem.* **2002**, *12*, 1664.
(37) Mohino, F.; Diaz, I.; Perez-Pariente, J.; Sastre, E. *Stud. Surf. Sci. Catal.* **2002**, *142*, 1275.
(38) Yang, Q.; Kapoor, M. P.; Inagaki, S. *J. Am. Chem. Soc.* **2002**, *124*, 9694.
(39) Dufaud, V.; Davis, M. E. *J. Am. Chem. Soc.* **2003**, *125*, 9403.
(40) Stein, A.; Melde, B.; Schroden, R. C. *Adv. Mater.* **2000**, *12*, 1403.
(41) Yang, Q.; Kapoor, M. P.; Inagaki, S.; Shirokura, N.; Kondo, J. N.; Domen, K. *J. Mol. Catal. A: Chem.* **2005**, *230*, 85.
(42) Esquivel, D.; Jimenez-Sanchidrian, C.; Romero-Salguero, F. J. *J. Mater. Chem.* **2011**, *21*, 724−733.
(43) Lim, M. H.; Blanford, C. F.; Stein, A. *J. Am. Chem. Soc.* **1997**, *119*, 4090.
(44) Anwander, R.; Nagi, I.; Widenmeyer, M.; Engelhardt, G.; Groeger, O.; Palm, C.; Röser, T. *J. Phys. Chem. B.* **2000**, *104*, 3532.
(45) Asefa, T.; Kruk, M.; MacLachlan, M. J.; Coombs, N.; Grondey, H.; Jaroniec, M.; Ozin, G. A. *J. Am. Chem. Soc.* **2001**, *123*, 8520.
(46) Nakajima, K.; Tomita, I.; Hara, M.; Hayashi, S.; Domen, K.; Kondo, J. N. *Adv. Mater.* **2005**, *17*, 1839.
(47) Sasidharan, M.; Fujita, S.; Ohashi, M.; Goto, Y.; Nakashima, K.; Inagaki, S. *Chem. Commun.* **2011**, *47*, 10422.
(48) Yoneda, G. S.; Griffin, M. T.; Carlyle, D. W. *J. Org. Chem.* **1975**, *40*, 375.
(49) Davis, S. R.; Brough, A. R.; Atkinson, A. *J. Non-Cryst. Solids* **2003**, *315*, 197.
(50) Bribes, J. L.; Elboukari, M.; Maillols, J. *J. Raman Spectrosc.* **1991**, *22*, 275.
(51) Sasidharan, M.; Wu, P.; Tatsumi, T. *J. Catal.* **2002**, *205*, 332.
(52) Temple, R. D. *J. Org. Chem.* **1970**, *35*, 1275.
(53) Sasidharan, M.; Wu, P.; Tatsumi, T. *J. Catal.* **2002**, *209*, 260.
(54) Schenck, R. T. E.; Kaizerman, S. J. *J. Am. Chem. Soc.* **1953**, *75*, 1636.
(55) Chevalier, P.; Corriu, R. J. P.; Delord, P.; Moreau, J. J. E.; Chiman, M. W. *New J. Chem.* **1998**, *22*, 423.
(56) Kirbaslar, S. I.; Baykal, Z. B.; Dramur, U. *Turk. J. Engin. Environ. Sci.* **2001**, *25*, 569−577.
(57) Lv, B. D.; Liu, G. P.; Dong, X. L.; Wei, W.; Jin, W. Q. *Ind. Eng. Chem. Res.* **2012**, *51*, 8079−8086.